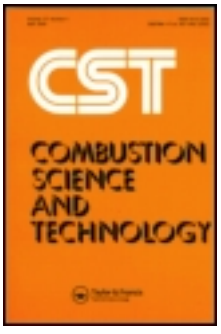

Combustion Science and Technology
Publication details, including instructions for authors and subscription information:
http://www.tandfonline.com/loi/gcst20

A Numerical Study of Reverse Smoldering

S.V. LEACH [a] , J. L. ELLZEY [a] & O. A. EZEKOYE [a]
[a] Department of Mechanical Engineering and Applied Research Laboratories , The University of Texas at Austin , Austin, TX, 78712
Published online: 05 Apr 2007.

To cite this article: S.V. LEACH , J. L. ELLZEY & O. A. EZEKOYE (1997) A Numerical Study of Reverse Smoldering, Combustion Science and Technology, 130:1-6, 247-267, DOI: 10.1080/00102209708935745

To link to this article: http://dx.doi.org/10.1080/00102209708935745

Combust. Sci. and Tech., 1997, Vol. 130, pp. 247–267
Reprints available directly from the publisher
Photocopying permitted by license only

A Numerical Study of Reverse Smoldering

S. V. LEACH, J. L. ELLZEY and O. A. EZEKOYE*

Department of Mechanical Engineering and Applied Research Laboratories, The University of Texas at Austin, Austin, TX 78712

(Received 12 March 1997; In final form 22 September 1997)

In this paper, we present the results from a one-dimensional transient model of reverse smoldering. Two step chemistry which includes oxidative and pyrolytic steps is used. In contrast to many earlier models, local thermal nonequilibrium between the solid and gas phase was allowed. Radiative transfer was included using the diffusion approximation. The solid energy, solid species, gas energy, oxygen species, and overall mass conservation equations were discretized in space using finite difference techniques and were solved using VODE (an ordinary differential equation integrator designed for stiff equations). The effects of inlet gas velocity, oxygen concentration, mass diffusion of oxygen, radiation, gas phase conduction, and volumetric heat transfer coefficient were studied using this model. Of particular interest were processes which led to extinction of the smolder wave. One example is the observation that the strong coupling between the volumetric heat transfer coefficient and inlet gas velocity modifies the smolder velocity and quenching dynamics of the wave.

Keywords: Reverse smolder; thermal nonequilibrium; quenching

INTRODUCTION

Smoldering is a slow flameless combustion process in a porous medium. Since the detailed chemistry is unknown for smoldering of most materials, smoldering is typically described by two competing reacting pathways, an endothermic solid pyrolytic reaction and an exothermic heterogeneous oxidative reaction. Both pathways form char, a high carbon material. In addition, exothermic heterogeneous oxidation of the char occurs forming ash.

The heat released during the heterogeneous oxidation of the solid is transferred toward the unreacted material by conduction, convection, and

*Corresponding author. E-mail: dezekoye@mail.utexas.edu.

radiation, supporting the propagation of the smolder reaction. The oxidizer, in turn, is transported to the reaction zone by diffusion and convection. These transport mechanisms influence the rate at which the smolder reaction propagates. Usually, smoldering combustion occurs at relatively low temperatures and propagates at low velocities.

Smoldering is customarily classified into forward and reverse configurations. In forward smolder propogation, reaction movement is in the same direction as the air flow. In reverse smolder, the oxidizer enters the reaction zone from opposite direction of the reaction propagation.

Smoldering combustion is a concern for fire safety reasons. First, smoldering reactions produce toxic combustion products which by themselves pose significant danger. Next, and perhaps, more importantly, smoldering reactions may transition to flaming reactions. A productive application of smoldering combustion is in waste incineration where the goal is to maintain the combustion wave so that the parameters of interest are far from the extinction limits.

Smoldering combustion of porous materials has been previously studied numerically, analytically, and experimentally. Most of the experimental analyses have focused on measuring the smolder rate under forced flow conditions. Ohlemiller (1985) provides a thorough review of smoldering combustion models prior to 1985 including that of Moussa *et al.* (1976); Summerfield *et al.* (1979) and Ohlemiller *et al.* (1979).

Moussa *et al.* (1976) modeled a cellulose cylinder smoldering in a stagnant atmosphere. Though the smolder behavior was two-dimensional in character, a one-dimensional model was used. The smolder reaction wave was split in two parts for subsequent analysis, an endothermic pyrolysis zone and a char oxidation zone. Later studies showed that the concept of a purely endothermic pyrolysis zone was probably incorrect and that competing oxidative and pyrolytic reactions exist. The summation of energy equations was used because of assumed local thermal equilibrium between gas and solid. The measured spreading speed and the maximum temperature of the smoldering zone were found to increase with increasing oxygen availability. The model predicted that extinguishment occurred with decreasing oxygen availablity.

A one-dimensional unsteady model of the forward propagation problem in cigarette smolder was developed by Summerfield *et al.* (1979). Only two reactions were included: non-oxidative pyrolysis and char oxidation. Radiation transfer in the solid was included by means of the "forward/reverse" approximation. The local gas and solid temperatures were not assumed to be equal. An increase in the bulk gas and bulk solid heat transfer

coefficient caused a nearly proportional increase in smolder wave speed. Suppression of radiative transfer caused a large increase in peak reaction zone temperature. Evidently, radiation constitutes a substantial mechanism for heat dissipation from this zone.

The most detailed model of reverse smolder propogation was done by Ohlemiller *et al.* (1979). Only two reactions were included, fuel oxidation and char oxidation. The endothermic pyrolytic reaction pathway was excluded. Gas and energy equations were combined on the assumption of local thermal equilibrium. Radiative transfer was included by means of the "forward/reverse" approximation. The model solutions correctly predict the qualitative trends for polyurethane foam of increasing smolder velocity and peak temperature with increased oxygen supply. The differing rates of increase depending on how oxygen supply is increased (higher gas velocity with fixed oxygen level or fixed velocity with increasing oxygen level) was also predicted. Quantitatively, the predicted temperatures and smolder velocities were low. Again the results imply that the smolder propagation process is oxygen supply rate limited. In reverse smoldering, char residue acts as an insulator against the only path for heat losses in one-dimensional propagation (losses from the originally ignited end of the fuel bed). Ohlemiller's model shows that this insulating char helps achieve self-sustaining smoldering.

Two-dimesional smoldering processes were modeled by Moallemi *et al.* (1993). A complete description of physical processes was included but a global single-step combustion reaction was assumed, thus a complete structure of the smoldering front was not predicted.

Di Blasi (1995) investigated a two-dimensional, unsteady, variable property model of the smoldering combustion of an insulating cellulosic bed in still air. This model accounted for a more complete description of the chemical processes. Both pyrolysis and heterogeneous oxidation of solid and char were taken into account. The structure of the smoldering wave was predicted and the effect of several parameters (heat and mass transfer coefficients from the exposed surface to the fuel and reaction rates) on the process was discussed.

An analytical model using activation energy asymptotics was developed by Dosanjh *et al.* (1987) to conduct a parametric investigation of reverse smoldering combustion. Key results were that the downstream temperature depends only on the initial oxygen mass flux and increases logarithmically with initial oxygen mass flux. The smolder velocity increased linearly with initial oxygen mass flux and at a fixed initial oxygen mass flux, increased with increasing initial oxygen mass fraction. Extinction occurred when all of

the energy released in the reaction zone was used to heat the incoming gas. As an extension of the work of Dosanjh *et al.* (1987); Schult *et al.* (1995) used large activation energy asymptotics to determine propagation velocity, burning temperature, final degree of fuel decomposition, and extinction limits for forced opposed flow smolder waves.

Fatehi and Kaviany (1994) examined theoretically and experimentally downward propagation of a combustion front in a packed bed of wood particles, with air supply from below. A single-step reaction, with a kinetic model of char oxidation as the dominant mechanism was used. Local thermal equilibrium was assumed, but a local chemical nonequilibrium between the solid and gas phases was allowed. The smolder speed, adiabatic temperature, and the extent of solid consumption were determined as functions of the entering air-pore velocity. Both oxygen and fuel limited regimes were studied. In the oxygen limited regime, the smolder speed, adiabatic temperature, the extent of solid consumption, and the thickness of the front all increased with increasing air-pore velocity. The reverse occurred in the fuel limited regime and extinction at high air-pore velocity was predicted.

Torero *et al.* (1993) experimentally studied the effect of a forced flow of oxidizer on the propagation of a smolder reaction through a highly porous polyurethane foam in a geometry that approximates one-dimensional reverse smolder propagation. The results confirm that the smolder process is controlled by the competition between the supply of oxidizer and the transfer of heat to and from the reaction zone. At low flow velocities, the smolder velocities and temperatures were relatively small and oxygen depletion was the controlling factor. Increasing flow velocities resulted in increased smolder velocities and temperatures due to the oxygen addition. The smolder velocities and temperatures reached a maximum however, and as the air velocity was further increased, the reaction became weaker and eventually died out due to convective cooling.

Lozinski and Buckmaster (1995) analyzed reverse smolder in a porous medium using asymptotic methods. Their model included endothermic pyrolysis as an attempt to indicate the possibility of quenching at high inlet gas velocities, a phenomenon not admitted in other analytical or numerical models, but observed experimentally.

The problem of smoldering combustion in porous fuel beds is very complicated both chemically and thermophysically. Kashiwagi and Nambu (1992) determined global kinetic constants for pyrolysis and oxidative degradation reactions for paper by thermal analysis. These kinetic constants and reactions will be used as an engineering approach to the chemical complexities. In this study, a one-dimensional transient reverse smoldering

combustion model is developed and used to build a body of knowledge about the quantitative interactions among the numerous model parameters. In particular, the effect of inlet gas velocity, oxygen concentration, mass diffusion of oxygen, radiation, gas phase conduction, and volumetric heat transfer coefficient will be studied using the numerical model. Local thermal nonequilibrium between the solid and gas phase is allowed in the model. Radiative transfer is included via the diffusion approximation.

NUMERICAL TECHNIQUE

Governing Equations

Solid Phase Equations

The governing equation in the solid is the heat equation:

$$\rho c \frac{\partial T}{\partial t} = \frac{\partial}{\partial x}\left(k_s \frac{\partial T}{\partial x} + \vec{q}_{rad}\right) - \omega_o \Delta h_o - \omega_p \Delta h_p + hA'''(T_g - T) \qquad (1)$$

where ρ is the bulk density, c is specific heat, k_s is solid conductivity, Δh_o and Δh_p are the enthalpies of reaction for oxidation and pyrolysis, hA''' is the product of the heat transfer coefficient and the surface area per unit volume, T_g is the gas temperature, and T is the solid temperature.

Also, a species conservation equation can be written to govern the evolution of the char mass fraction, y_c:

$$\frac{\partial(\rho y_c)}{\partial t} = \omega_o n_{c_1} + \omega_p n_{c_2} \qquad (2)$$

where ω_o and ω_p are the mass rates of production for oxidation and pyrolysis and n_{c1} and n_{c2} are stoichiometric coefficients.

Gas Phase Equations

The solid conversion process produces gases which flow through the solid pile. One-dimensional flow in the model is assumed. The gas phase continuity equation is:

$$\frac{\partial}{\partial t}(\rho_g \phi) + \frac{\partial}{\partial x}(\rho_g \phi u) = \phi[\omega_p n_{g_2} + \omega_o(n_{g_1} - n_{O_2})] \qquad (3)$$

where ϕ is porosity, and the subscript g is for gas.

The gas phase energy equation is:

$$\phi\rho_g c_{pg}\left(\frac{\partial T_g}{\partial t}+u\frac{\partial T_g}{\partial x}\right)=\phi k_g\frac{\partial^2 T_g}{\partial x^2}+hA'''(T-T_g) \tag{4}$$

where c_{pg} is the specific heat of gas. The oxygen species equation is:

$$\frac{\partial}{\partial t}(\rho_g\phi y_{O_2})+\frac{\partial}{\partial x}(\rho_g\phi u y_{O_2})+\frac{\partial}{\partial x}(\rho_g\phi y_{O_2}V_{O_2})=-\phi\omega_o n_{O_2} \tag{5}$$

where V_{O_2} is the diffusional velocity of oxygen given by

$$V_{O_2}=-D_{O_2m}\frac{\partial y_{O_2}}{\partial x} \tag{6}$$

where y_{O_2} is the mass fraction of oxygen and m denotes the mixture.

Property Definitions

It is convenient to define the char mass fraction as y_c and define the solid properties (ρ, ϕ, and k) in terms of this char mass fraction. Radiation heat transfer is modeled in the optically thick limit. For this limit, the radiative flux vector is proportional to the temperature gradient. The constant of proportionality may be thought of as "radiative conductivity". The total thermal conductivity is given as

$$k=k_{con}+k_{rad} \tag{7}$$

$$k_{con}=y_c k_c+(1-y_c)k_f \tag{8}$$

$$k_{rad}=16\sigma d T^3/3 \tag{9}$$

where

$$d=y_c d_c+(1-y_c)d_f \tag{10}$$

and σ is the Stefan-Boltzmann constant, T is the solid temperature, and d is the pore diameter.

Kinetics

A three-step reaction model that allows for char formation and oxidation given by Rogers and Ohlemiller (1980) is as follows:

Exothermic Thermal Oxidation

$$1g(\text{fuel}) + n_{O_1}O_2 \rightarrow n_{c1}(\text{char}) + n_{g1}(\text{gases}) \tag{11a}$$

Endothermic Pyrolysis

$$1g(\text{fuel}) \rightarrow n_{c2}(\text{char}) + n_{g2}(\text{gases}) \tag{11b}$$

Exothermic Char Oxidation

$$1g(\text{char}) + n_{O_3}O_2 \rightarrow n_{a3(\text{ash})} + n_{g3}(\text{gases}) \tag{11c}$$

Ohlemiller and Lucca (1983) observed that the slower kinetics of the second stage (char oxidation) caused it to lose out in the competition for the available oxygen and the smolder wave moved forward powered by the less energetic first stage. Therefore, neglecting the second stage reaction in the model may be acceptable for the reverse smoldering case. Thus, the present model allows only for char formation ((11a) and (11b)). At high flow velocities and/or high oxygen concentrations, some oxygen may still be available for char oxidation. As char oxidation is highly exothermic, the temperature profiles may be affected and consequently the smoldering characteristics may be slightly different from those presented which exclude the char oxidation reaction. The mass rates of production are similar to those given by Kashiwagi and Nambu (1992) and are of the following form:

Thermal Oxidation

$$\omega_o = (1 - y_c)^f (y_{ox})^m A_O e^{\frac{E_{aO}}{RT}} \tag{12a}$$

Pyrolysis

$$\omega_p = (1 - y_c)^g A_p e^{\frac{E_{ap}}{RT}} \tag{12b}$$

where y_c is the char fraction, y_{ox} is the mass fraction of oxygen, A is the preexponential frequency factor, E_a is the activation energy, and f, m, and g are empirically determined exponents.

Boundary and Initial Conditions

The geometry is shown in Figure 1. The left boundary is at a fixed temperature, T_w. Air flows through the right boundary into the fuel bed. The smolder propogates from left to right.

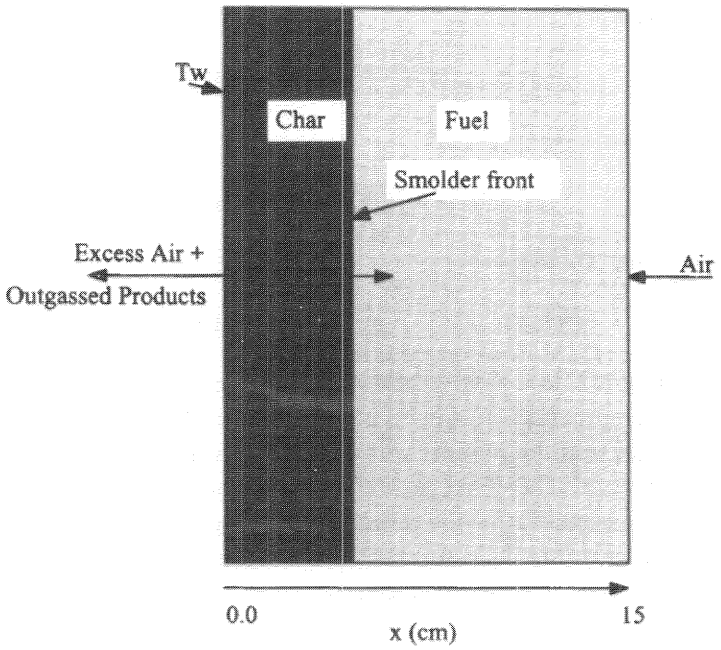

FIGURE 1 Sketch of the reverse smoldering configuration with forced air flow. The left side ($x = 0$ cm) is held at 600 K. Air (23.5% O_2 by mass) is forced through the right side ($x = 15$ cm) at 0.17 cm/sec.

At $x = 0$,

$$T = T_w, \quad \frac{\partial T_g}{\partial x} = 0, \quad \frac{\partial y_{O_2}}{\partial x} = 0 \tag{13}$$

At $x = l$,

$$\frac{\partial T}{\partial x} = 0, \quad T_g = T_{g\,in}, \quad y_{O_2} = y_{O_2\,in}, \quad u = u_{in} \tag{14}$$

At $t = 0$,

$$T = T_{in}, \quad T_g = T_{g_{in}}, \quad y_{O_2} = y_{O_2\,in}, \quad y_c = 0 \tag{15}$$

Solution Method

The solid energy, solid species, gas energy, and oxygen species equations were rearranged and discretized in space using finite difference techniques. For this problem, the code VODE (Brown *et al.*, 1989) is used. VODE is an

ordinary differential equation integrator designed for stiff equations and is frequently used in applications involving chemical kinetics.

In this model, the pressure drop across the pile was assumed negligible. In order to clarify when this assumption is valid, the conservation of momentum equation was non-dimensionalized. It was found that for high porosity, the momentum equation (i.e., the Darcy law) becomes trivial. Thus, the gas velocity is solved for directly using mass conservation.

Calculations were performed for 50 to 400 grid points for the base case to ensure grid independence of the results. Time step selection is controlled by VODE. We tested several different error criterion (relative tolerances) to ensure that time stepping is accurate.

RESULTS

A Base Case

In this section, we present the results from our one-dimensional simulations of reverse smolder. We discuss a base case in which the parameters were chosen to represent the smoldering of a porous bed of polyurethane foam. We were unable to obtain kinetic parameters for polyurethane foam and therefore used those for cellulosic paper. In Ohlemiller's review paper (1985), he noted that smolder velocities do not vary greatly in spite of wide variations in fuel type and configuration. These parameters are listed in Table I. We then vary the inlet gas velocity and oxygen concentration. In addition, we examine the importance of mass diffusion, radiation, gas phase conduction, and volumetric heat transfer coefficient on the smoldering process.

The variation of temperature, char fraction, and oxygen concentration are shown in Figure 2a, and the variation of gas velocity and heat release in Figure 2b for the base case. Initially, the solid is at 300 K. The temperature at the left boundary is increased to and held at 600 K. For reverse smoldering, a wave structure similar to a premixed laminar flame is observed in that the fuel and oxidizer are intermingled as they enter the reaction zone and need only a sufficient temperature to initiate the reaction. So, the rate of reverse smolder propagation is strongly determined by the rate of heat transfer to the incoming fuel and oxidizer. The rate of heat transfer is limited by the rate at which heat is evolved. Heat generation occurs in the exothermic oxidative reaction and this reaction depends on the oxygen supply. In this case, the oxygen is not completely consumed by the end of the reaction zone. At time = 850 sec, the location of the smolder front

TABLE I Base case in parameters

Property	*Value in mks units*	*Value in cgs units*	*Reference*
hA'''	1000 W/(m^{3}K)	1e4 g/(cm K s^3)	Florio *et al.* (1989)
Δh_O	−5700 J/g	−5.7e10 erg/g	Kashiwagi & Nambu (1992)
Δh_p	570 J/g	5.7e9 erg/g	Kashiwagi & Nambu (1992)
n_{O1}	0.41	0.41	Kashiwagi & Nambu (1992)
n_{c1}	0.21	0.21	Kashiwagi & Nambu (1992)
n_{c2}	0.24	0.24	Kashiwagi & Nambu (1992)
A_o	2.5e12 1/sec	2.5e12 1/sec	Kashiwagi & Nambu (1992)
$E_{a\,o}/R$	19,244.65 K	19,244.65 K	Kashiwagi & Nambu (1992)
f	1.3	1.3	Kashiwagi & Nambu (1992)
m	0.5	0.5	Kashiwagi & Nambu (1992)
A_p	2e17 1/sec	2e17 1/sec	Kashiwagi & Nambu (1992)
$E_{a\,p}/R$	26,461.39 K	26,461.39 K	Kashiwagi & Nambu (1992)
g	1.8	1.8	Kashiwagi & Nambu (1992)
k_c	4.2e-2 W/mk	4200 erg/(s cm K)	Di Blasi (1995)
k_f	6.3e-2 W/mk	6300 erg/(s cm K)	Di Blasi (1995)
d_f	5e-5 m	0.005 cm	Torero (1993)
d_c	8e-5 m	0.008 cm	estimated
ρ_c	10 kg/m^3	0.01 g/cm^3	estimated
ρ_f	26.5 kg/m^3	0.0265 g/cm^3	Torero (1993)
c_c	1.1 kJ/(kgK)	1.1e7 erg/gK	Di Blasi (1995)
c_f	1.7 kJ/(kgK)	1.7e7 erg/gK	Torero (1993)
k_g	25.77 e-3 W/mK	2577 erg/(s cm K)	Di Blasi (1995)
ϕ_f	0.975	0.975	Torero (1993)
ϕ_c	0.975	0.975	estimated
$D_O 2m$	4.53e3 m^2/s	0.453 cm^2/s	Torero (1993)
T_w	600K	600K	
$T_{g\,in}$	300K	300K	
$y_{O_2 in}$	0.235	0.235	
u_{in}	0.0017 m/s	0.17 cm/s	Torero (1993)

is approximately $x = 3$ cm as indicated by the maximum heat release rate (Fig. 2b). Some of the heat generated by the reactions is transferred to the unburned fuel, causing the smoldering reaction to propagate through the pile. We estimate this smoldering front velocity by measuring the distance between the locations of peak heat release at two different times and dividing by the change in time. The smolder velocity is approximately 0.006 cm/sec.

From the graphs, it can be seen that a steady propagation rate is reached. At approximately $x = 12$ cm, the reactions stop as indicated by the heat release in Figure 2b. A peak temperature in the smolder zone is approximately 575 K.

The extinction process is complicated and we are currently investigating this phenomenon. A literature review and our current numerical studies indicate several possible mechanisms of extinction. These include convective heat transfer from the solid to the gas, "flammability" type limits, and the endothermic pyrolytic reaction.

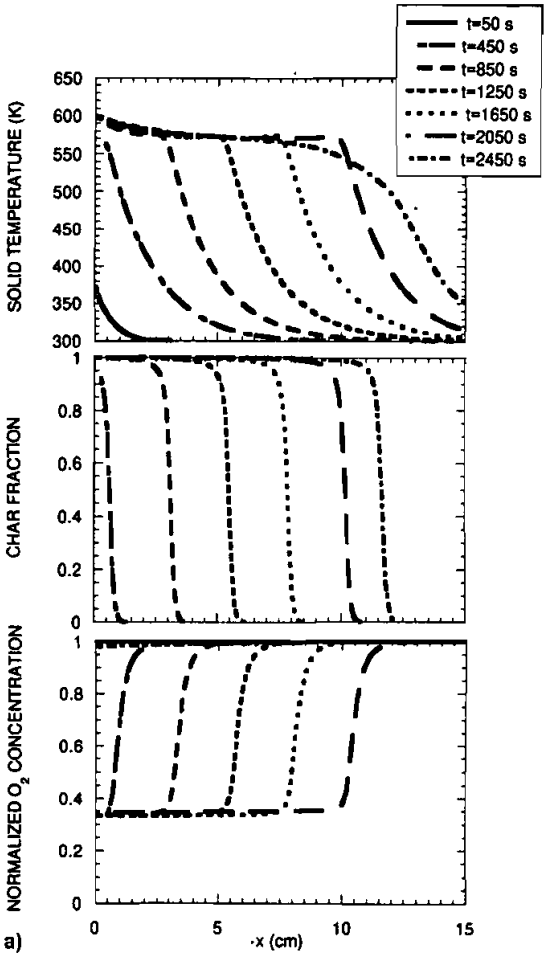

FIGURE 2a Solid temperature, char fraction, and normalized oxygen concentration vs. distance plotted in 400 sec increments for the base case of reverse smoldering. The solid temperature is brought to and then held at 600 K at $x = 0$ cm and is insulated at $x = 15$ cm. Air at 300 K is forced at 0.17 cm/sec at $x = 15$ cm.

The air velocity into the fuel at $x = 15$ cm is specified at 0.17 cm/sec (Fig. 2b). As the air flows through the solid (from right to left), it is heated by convective heat transfer from the solid. The gas density decreases resulting in an increased velocity. Gasification in the reaction zone also causes the gas velocity to increase. The total increase of the gas velocity due to these two effects is shown in Figure 2b.

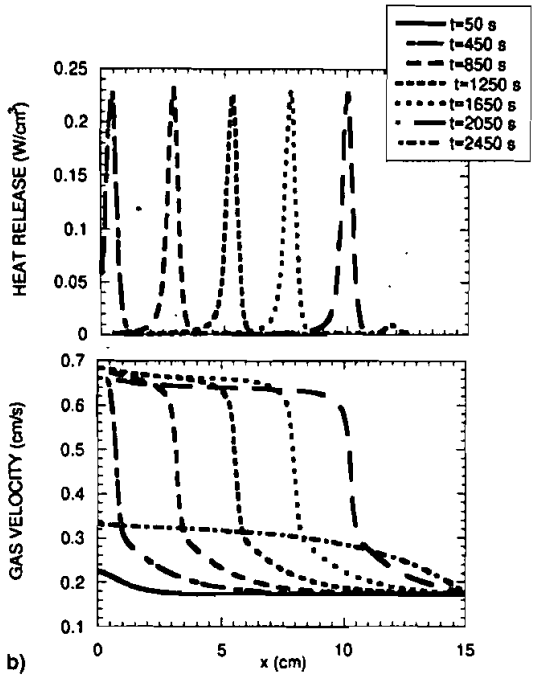

FIGURE 2b Heat release and gas velocity vs distance plotted in 400 sec increments for the base case of reverse smoldering. The solid temperature is brought to and then held at 600 K at $x = 0$ cm and is insulated at $x = 15$ cm. Air at 300 K is forced at 0.17 cm/sec at $x = 15$ cm.

Effect of Inlet Gas Velocity

For this case, we used all of the parameters for the base case except that the inlet gas velocity was varied from 0.03 cm/sec to 0.41 cm/sec. From these simulations, we determined the smolder velocity, distance to extinguishment, maximum temperature in the smolder zone, and peak steady state heat release (Tab. II).

These results show that increasing the inlet gas velocity from 0.03 cm/sec to 0.09 cm/sec increased the smolder rate, the distance to extinguishment, and the maximum temperature. As the inlet gas velocity is further increased to 0.17 cm/sec, the smolder velocity, the distance to extinguishment, and the maximum temperature remained relatively constant. Further increases in the inlet gas velocity resulted in a decreased distance to extinguishment and eventually a smolder wave would not propogate at all due to convective cooling. The steady state peak heat release rate always increased with increasing inlet gas velocity. In Figure 3, we compare our calculated smolder

TABLE II Effect of inlet gas velocity on smolder velocity, distance to extinguishment, peak temperature at the end of the smolder zone, and peak steady state heat release

U_{in} (cm/s)	$V_{smolder}$ (cm/s)	$X_{extinguish}$ (cm)	$T_{maximum}$ (K)	Steady peak heat release (W/cm^3)
0.030	0.0030	11.0	545	0.045
0.048	0.0045	11.8	560	0.073
0.090	0.0060	12.0	570	0.135
0.130	0.0060	12.0	573	0.180
0.170	0.0060	12.0	575	0.220
0.200	0.0060	11.5	575	0.250
0.231	0.0060	4.0	575	0.275
0.250	never propagated steadily			
0.280	never propagated steadily			
0.410	never propagated steadily			

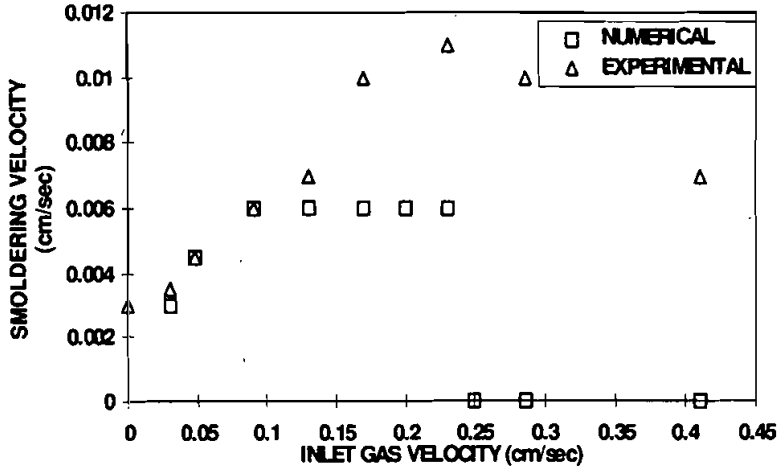

FIGURE 3 Smoldering velocity vs. inlet gas velocity. Experimental data is taken from Torero *et al.* (1993).

velocities to the experimental results of Torero *et al.* (1993). At low inlet velocities, either fortuitously or by Ohlemiller's observations (1985) that smolder velocities do not vary greatly in spite of wide variation in fuel type, we were able to match the smolder velocity without tuning the material properties. At higher velocities, the model underpredicts the smolder velocity but still shows the correct trend. For inlet velocities greater than 0.25 cm/sec, the smolder front extinguishes. The experiment of Torero *et al.* (1993) also show that the front extinguishes at inlet velocities greater than 0.41 cm/sec.

Effect of Inlet Oxygen Concentration

For this case, we used the parameters from the base case but varied the inlet oxygen concentration from 0.1 to 1.0. The smolder velocity, distance to extinguishment, peak temperature at the end of the smolder zone, and peak steady state heat release for these computations are shown in Table III.

We found that increasing the inlet oxygen concentration resulted in an increased smolder velocity, distance to exitnguishment, peak temperature, and steady state peak heat release. Figure 4 shows that increasing the oxygen supply will lead to an increased reverse smolder rate. This result is consistent with the reports of Dosanjh *et al.* (1987). At an inlet oxygen concentration of 0.1, the reaction immediately started to extinguish and never propagated steadily. Increasing the initial oxygen concentration allowed the smolder wave to propagate further and more quickly. With an inlet oxygen concentration of 0.5 and higher, the smolder wave propagated through the entire 15 cm pile of foam.

TABLE III Effect of oxygen concentration on smolder velocity, distance to extinguishment, peak temperature at the end of the smolder zone, and peak steady state heat release

$y_{O_2 in}$ (cm/s)	$V_{smolder}$ (cm)	$X_{extinguish}$ (K)	T	steady peak heat release (W/cm^3)
0.100	0.0015	1.40	–	never propagated steadily
0.235	0.0060	12.0	575	0.220
0.300	0.0080	13.5	580	0.350
0.500	0.0135	–	590	0.700
0.700	0.0180	–	600	1.100
0.900	0.0220	–	605	1.600
1.000	0.0250	–	605	1.800

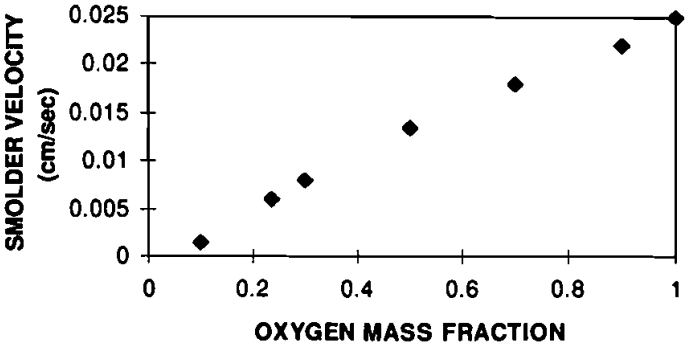

FIGURE 4 Smolder velocity vs. oxygen mass fraction.

Effect of Including Mass Diffusion of Oxygen, Gas Phase Conduction, and Radiation

In these simulations, we examined the importance of mass diffusion of oxygen, gas phase conduction, and radiation. The base case included all three of these processes. The same base case was simulated for conditions when one of the three processes was excluded. Finally, the base case was run without any of the three processes. These results are shown in Table IV.

When mass diffusion of oxygen was not included, the smolder wave velocity increased. Increases in the reaction rate necessarily imply an increase in the wave velocity. In decreasing the diffusion coefficient of oxygen, the upstream influence of the reaction zone is not as significant and more oxygen is present in the reaction zone. As a result, the reaction rate is increased.

When radiative transfer was not included, the smolder velocity was the same as in the base case and the reaction was extinguished at about the same location as in the base case, showing that radiation is a weak mechanism for heat transfer from the reaction zone, at least when the diffusion approximation is used and pore diameters are small. For larger pore diameters, radiation will become more important.

Gas phase conduction also played an important role in the smolder wave's velocity and extinguishment. When gas phase conduction was not included, the smolder velocity was lower and the wave propagated through the entire 15 cm pile. It appears that extinguishment occurs because heat is conducted away from the solid through the gas. Gas phase conduction is also a substantial mechanism for heat transfer from the reaction zone.

Overall, we consider two of these cases to be driven by an effective Lewis number modification to the smolder wave speed. Neglecting mass diffusion

TABLE IV Effect of mass diffusion of oxygen, gas phase conduction, and radiation on smolder velocity, distance to extinguishment, peak temperature at the end of the smolder zone, and peak steady state heat release

	$V_{smolder}$ (cm/s)	$X_{extinguish}$ (cm)	T (K)	steady peak heat release (W/cm^3)
Base case including mass diffusion of O_2, radiation, and gas phase conduction	0.0060	12.0	575	0.230
No mass diffusion of O_2	0.0073	12.5	575	0.300
No radiation in the conductivity	0.0060	11.5	575	0.230
No gas phase conduction	0.0045	–	585	0.230
No mass diffusion of O_2, no radiation, no gas phase conduction	0.0060	–	585	0.300

of oxygen tends to increase the effective "mixture" Lewis number while neglecting radiative transfer tends to decrease the effective Lewis number. Similar to premixed flame analysis, the smolder wave speed is increased by increasing the Lewis number.

The Effect of Volumetric Heat Transfer Coefficient of Smolder Velocity

The existence of local thermal equilibrium has been an assumption in many previous numerical models (Moussa *et al.* (1976); Ohlemiller *et al.* (1979); Moallemi *et al.* (1993) and Di Blasi (1995)) and analytical models (Dosanjh *et al.* (1987); Fatehi and Kaviany (1994); Lozinski and Buckmaster (1995) and Schult *et al.* (1995)) dealing with the thermal response of smoldering materials. However, since the thermal response of these systems is highly transient, some researchers have suggested that large deviations from local thermal equilibrium do exist (Florio *et al.*, 1989). Thermal decomposition is enhanced with increased departure from thermal equilibrium since the solid retains more heat.

In order to see when the simplifying assumption of local thermal equilibrium would be valid, we used a range of volumetric heat transfer coefficients (10 to 100,000 W/m^3K) for several different inlet gas velocities (0.03, 0.048, 0.17, 0.28, and 0.41 cm/sec). This examination of the effect of volumetric heat transfer coefficient neglects all of the processes that must be affected when the transfer coefficient is varied over the wide range chosen. In particular, such a wide range might require varying the pore size of the fuel bed. The results are shown in Table V and Figure 5.

For low inlet gas velocities (0.03 and 0.048 cm/sec), varying the heat transfer coefficient did not result in a significant change in smolder velocity,

TABLE V Effect of volumetric heat transfer coefficient on smolder velocity for several inlet gas velocities. Smolder velocities are in cm/sec. Experimental data is taken from Torero *et al.* (1993)

hA''' (W/m^3K)	Inlet Gas Velocity (cm/sec)	0.03	0.048	0.17	0.28	0.41
10		0.0039	0.0045	0.0091	0.012	0.014
100		0.0033	0.0045	0.0075	0.009	0.010
1000		0.0033	0.0045	0.006	did not propagate	did not propagate
10000		0.0033	0.0045	0.006	did not propagate	did not propagate
100,000		0.0030	0.0045	0.006	did not propagate	did not propagate
experimental		0.0035	0.0045	0.01	0.01	0.007

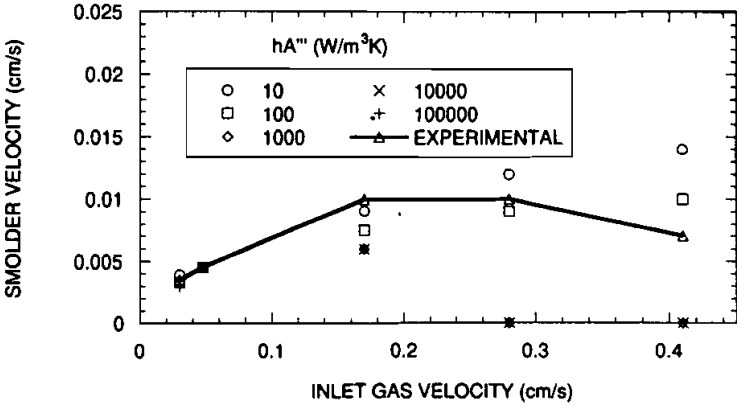

FIGURE 5 The effect of volumetric heat transfer coefficient on smolder velocity is shown for several different inlet gas velocities. Experimental data is taken from Torero *et al.* (1993).

implying that thermal equilibrium is a valid assumption for low inlet gas velocities. The calculated smolder velocity agreed very well with what was reported experimentally (Torero *et al.*).

However, as the inlet gas velocity was increase to 0.17 cm/sec, varying the volumetric heat transfer coefficient had a significant impact on the smolder velocity. Increasing the volumetric heat transfer coefficient from 10 to 100 to 1000 W/m^{3}K resulted in a decrease of the smolder wave velocity from 0.0091 to 0.0075 to 0.006 cm/sec. With lower volumetric heat transfer coefficients, the solid is retaining more heat which promotes higher reaction rates and therefore, higher smolder wave velocities. With lower heat transfer coefficients, the smolder velocity is closer to what was observed experimentally. Increasing the volumetric heat transfer coefficient beyond 1000 W/m^{3}K, however, did not result in a change of the smolder wave velocity. This suggests that thermal equilibrium was attained and further increases in volumetric heat transfer coefficient had no impact.

For inlet gas velocities of 0.28 cm/sec and 0.41 cm/sec, a smolder wave would propagate only for low volumetric heat transfer coefficients (10 W/m^{3}K and 100 W/m^{3}K). As the heat transfer coefficient was raised above these values, a sufficient solid temperature to allow the smolder wave to propagate was not reached.

At high values of the volumetric heat transfer coefficient, the solid and gas temperatures approach each other and thermal equilibrium may be assumed. Once thermal equilibrium between the solid and gas has been attained further increases in the heat transfer coefficient will have no effect.

The volumetric heat transfer coefficient is related to the velocity (Florio *et al.*) and at low velocities we expect a small volumetric heat transfer coefficient. Our results show, however, that for low inlet velocities, (0.03 cm/sec and 0.048 cm/sec), changes in the heat transfer coefficient do not affect the smolder velocity. Therefore, thermal equilibrium is a valid assumption. For an inlet gas velocity of 0.17 cm/sec, the smolder velocity is affected by the volumetric heat transfer coefficient. Thermal equilibrium should not be assumed unless the volumetric heat transfer coefficient is greater than 1000 W/m^3K. At an inlet gas velocity of 0.28 cm/sec, the smolder velocity was affected by all values of the volumetric heat transfer coefficient. Thermal equilibrium should not be assumed in this case. At high values of the volumetric heat transfer coefficient (greater than 1000 W/m^3K), the solid is not able to retain enough heat for the chemical reactions to occur. This agrees with the experimental observations of Torero *et al.*, who report that the smolder velocity increases with inlet gas velocity to a maximum, and then decreases until quenching occurs.

EXTINCTION

Our model is able to predict extinction for certain situations because thermal non-equilibrium is allowed. Results in this paper show that extinction occurs at high inlet gas velocities. This was also observed experimentally by Torero *et al.* (1993). The heat transfer coefficient is increased with increasing air flow velocity (Florio *et al.*, 1989) and therefore allows more heat to be transferred from the solid with increasing air flow velocity. It is the solid temperature which drives the reactions. With increasing gas velocity and heat transfer coefficient, the solid is eventually not able to attain sufficient temperature to sustain the reactions.

In solid deficient conditions (solid fuel is completely consumed and oxygen is not), the flow of oxidizer does not influence the heat release in the reaction. Increased air velocity lowers the combustion temperature (more heat is needed to heat the incoming gas). Significantly large gas fluxes cause extinction.

Pyrolysis could also play an important role in quenching. Pyrolysis could enhance extinction in several ways. First of all, the pyrolysis reaction is endothermic, taking heat away from the system. Secondly, pyrolysis does not consume any oxygen, leaving more to cool the reaction zone. In addition, pyrolysis consumes some of the fuel that could have been oxidized exothermically.

CONCLUSIONS

Using the global kinetic constants for pyrolysis and oxidative degradation of paper determined by Kashiwagi and Nambu (1992), a one-dimensional transient model of reverse smoldering was developed for high porosity and permeability conditions. Local thermal non-equilibrium between the solid and gas phase was allowed in the model, and this appears to uncover the possibility of heat transfer induced extinction. Radiative transfer was included in the optically thick limit. The effects of inlet gas velocity, oxygen concentration, mass diffusion of oxygen, radiation, gas phase conduction, and volumetric heat transfer coefficient were studied using this model.

A base case was obtained using realistic property values from the literature. In order to determine the effect of inlet gas velocity on the smoldering process, the same base case was used and the inlet gas velocity was varied. We observed that increasing the inlet gas velocity first resulted in an increased smolder rate, increased distance to extinguishment, and increased peak smoldering temperature. As the inlet gas velocity was further increased, the smolder velocity leveled off, distance to extinguishment decreased, and peak temperature decreased. The steady state peak heat release always increased with increasing inlet gas velocity.

The same base case was used and the inlet oxygen concentration was varied. It was found that increasing the inlet oxygen concentration resulted in an increased smolder velocity, distance to extinguishment, peak temperature, and steady state peak heat release. At very low inlet oxygen concentrations, the reaction immediately started to extinguish and never propagated steadily. Increasing the initial oxygen concentration allowed the smolder wave to propagate further and more quickly.

Also, our calculations show that mass diffusion of oxygen decreased the smolder velocity, radiation had little effect, and gas phase conduction increased the smolder wave velocity. A Lewis number analogy compares smoldering to premixed flames adding insight into how these phenomena influence smoldering characteristics.

The effect of volumetric heat transfer coefficient on the smolder velocity was also studied and it was found that for low inlet gas velocities, the assumption of thermal equilibrium could be justified. At higher inlet gas velocities, the volumetric heat transfer coefficient has a larger effect on the smolder velocity, and thermal equilibrium should not be assumed. The volumetric heat transfer coefficient should increase with increasing inlet gas velocity. Quenching occurs when the volumetric heat transfer coefficient is

so high that the solid is not able to retain enough heat for the chemical reactions to occur.

Acknowledgements

This work was sponsored by the Applied Research Laboratories at the University of Texas at Austin through the Office of Naval Research.

NOMENCLATURE

A	frequency factor
c	specific heat
D	diffusion coefficient
d	pore diameter
E_a	activation energy
f	exponent
g	exponent
hA'''	volumetric heat transfer coefficient
k	conductivity
m	exponent
n	stoichiometric coefficient
R	gas constant
T	temperature
u	gas velocity
V	diffusion gas velocity
x	coordinate
y	mass fraction

Greek Symbols

Δh	enthalpy of reaction
ϕ	porosity
ρ	density
σ	Stefan-Boltzmann constant
ω	mass rate of production

Subscripts

a	ash
c	char

f	fuel
g	gas
in	initial
o	oxidation
O_2	oxygen
p	pyrolysis
s	solid
w	wall

References

Brown, P. N., Byrne, G. D. and Hindmarsh, A. C. (1989) VODE: A Variable Coefficient ODE solver. *SIAM Journal of Scientific and Statistical Computing*, **10**, 1038–1051.

Di Blasi, C. (1995) Mechanisms of Two-Dimensional Smoldering Propagation Through Packed Fuel Beds. *Combust. Sci. and Tech.*, **106**, 103–124.

Dosanjh, S., Pagni, P. and Fernandez-Pello, A. (1987) Forced Cocurrent Smoldering Combustion. *Combustion and Flame*, **68**, 131–142.

Fatehi, M. and Kaviany, M. (1994) Adiabatic Reverse Combustion in a Packed Bed. *Combustion and Flame*, **99**, 1–17.

Florio, J., Henderson, J., Test, F. and Hariharan, R. (1989) Experimental Determination of Volumetric Heat Transfer Coefficients in Decomposing Polymer Composites. *Porous Media, Mixtures and Multiphase Heat Transfer*, Vafai *et al.*, eds HTD **117**.

Kashiwagi, T. and Nambu, H. (1992) Global Constants for Thermal Oxidative Degradation of a Cellulosic paper. *Combustion and Flame*, **88**, 345–368.

Lozinski, D. and Buckmaster, J. (1995) Quenching of Reverse Smolder. *Combustion and Flame*, **102**, 87–100.

Moallemi, M., Zhang, H. and Kumar, S. (1993) Numerical Modeling of Two-Dimensional Smoldering Processes. *Combustion and Flame*, **95**, 170–182.

Moussa, N., Toong, T. and Garris, C. (1976) *Sixteenth Symposium (International) on Combustion*, The Combustion Institute, Pittsburgh, Pa., p.1447.

Ohlemiller, T. J. (1985) Modeling of Smoldering Combustion Propagation. *Progress in Energy and Combustion Science*, **11**, 227–310.

Ohlemiller, T. J., Bellan, J. and Rogers, F. (1979) A Model of Smoldering Combustion Applied to Flexible Polyurethane Foams. *Combustible and Flame*, **36**, 197–215.

Ohlemiller, T. J. and Lucca, D. A. (1983) An Experimental Comparison of Forward and Reverse Smolder Propagation in Permeable Fuel Beds. *Combustion and Flame*, **54**, 131–147.

Rogers, F. E. and Ohlemiller, T. J. (1980) Cellulosic Insulation Material 1. Overall Degradation Kinetics and Reaction Rates. *Combustion Science and Technology*, **24**, 129–137.

Schult, D., Matkowsky, B. and Volpert, V. (1995) Propagation and Extinction of Forced Opposed Flow Smolder Waves. *Combustion and Flame*, **101**, 471–490.

Summerfield, M., Ohlemiller, T. and Sandusky, H. (1979) *Combustion and Flame*, **33**, 263.

Torero, J. L., Fernandez-Pello, A. C. and Kitano, M. (1993) Opposed Forced Flow Smoldering of Polyurethane Foam. *Combust., Sci. and Tech.*, **91**, 95–117.